

SHAPING THE CO SNOWLINE IN PROTOPLANETARY DISKS

S. Gavino¹, J. Kobus², A. Dutrey³, S. Guilloteau³, S. Wolf², J. K. J orgensen¹ and R. Sharma¹

Abstract. Characterizing the dust thermal structure in protoplanetary disks is a fundamental task as the dust temperature can affect both the disk chemical evolution and planet formation. It is a challenging task, however, since the temperature is strongly dependent on many parameters, including the grain size distribution. We investigate the effects of the radiative interactions between multiple dust populations on the CO distribution using dedicated thermochemical disk models. We find that the interaction of the dust scattered light between at least two dust grain populations can produce a complex temperature structure. In particular, the scattered light is sufficient to significantly raise the temperature of micron-sized grains in the midplane. This results in the splitting of the CO snowline that can strongly reshuffle the distribution of both CO in the gas-phase and on the grain surface.

Keywords: protoplanetary disks, astrochemistry, radiative transfer, planet formation

1 Introduction

It is now expected that grain growth in protoplanetary disks occurs fast (e.g. Testi et al. 2014; Harsono et al. 2018; Ohashi et al. 2023), implying the presence of a large grain-size range. The extinction opacities are therefore difficult to characterize. Most recent studies consider a dust model composed of two-grain populations, a small dust population and a large dust population (e.g. Du & Bergin 2014; Ballering et al. 2021; Zhang et al. 2021) meant to fit observationally constrained evidence of grain growth and size-dependent distribution (Gr afe et al. 2013; P erez et al. 2015; Villenave et al. 2020). Each population has its opacity averaged over a given size range, but a single resulting temperature is usually extracted for chemistry post-processes. However, since surface chemistry is strongly sensitive to dust surface temperatures, this treatment may overlook possible chemical effects by not considering the two dust structures independently. Indeed, real disks are most likely composed of grains of multiple sizes with independent optical properties, resulting in a complex radiative interaction between each grain species, and in a size-dependent temperature structure. In this work, we reproduce a typical two-size dust model as in recent studies, but we keep the dust structures independent so we can analyze the size-dependent temperature structures in the disk computed using dust continuum radiative transfer simulations and investigate the effect on the resulting CO distribution by treating the various dust populations simultaneously and independently in chemistry post-processes.

2 Model

2.1 Disk physical structure

The model is a static protoplanetary disks, consisting of a 2-D parametric smooth, axisymmetric and geometrically flared structure. Additionally, only passive heating is assumed. The disk is in Keplerian rotation. A more detailed description is given in Gavino et al. (2021). The radial gas surface density follows a simple truncated power-law,

¹ Niels Bohr Institute and Centre for Star and Planet Formation, University of Copenhagen,  ster Voldgade 5-7, 1350, Copenhagen K, Denmark

² University of Kiel, Institute of Theoretical Physics and Astrophysics, Leibnizstrasse 15, 24118 Kiel, Germany

³ Laboratoire d'Astrophysique de Bordeaux, Universit  de Bordeaux, CNRS, B18N, All e Geoffroy Saint-Hilaire, F-33615 Pessac

$$\Sigma_g = \Sigma_{g,0} \left(\frac{r}{R_0} \right)^{-p}. \quad (2.1)$$

we allow for a warmer disk atmosphere using the formulation of Williams & Best (2014)

$$T_g(r, z) = T_{\text{mid}}(r) + (T_{\text{atm}}(r) - T_{\text{mid}}(r)) \sin \left(\frac{\pi z}{2z_{\text{atm}}} \right)^{2\sigma} \quad (2.2)$$

We solve the gas density by considering the (non-isothermal) vertical hydrostatic pressure equilibrium, that we solve iteratively following Hersant et al. (2009),

$$\ln(\rho_g(z_i)) = \ln(\rho_g(z_i - 1)) - (\Omega^2 \frac{\mu m_H}{k_B T_g(z_i)} + (\ln(T_g(z_i)) - \ln(T_g(z_{i-1})))) \quad (2.3)$$

The vertical density distribution of any dust component is defined by a vertical Gaussian profile. The dust scale height is size-dependent and is defined following (see Youdin & Lithwick 2007; Fromang & Nelson 2009; Dong et al. 2015),

$$H_d(a, r) = H_g(r) \frac{1}{\sqrt{1 + \text{St} \frac{S_c}{\alpha}}} \quad (2.4)$$

where S_c is the Schmidt number and α the turbulent viscosity coefficient, set to 1 and 0.01, respectively, in the whole study. The dust scale height therefore represents a fraction of the gas scale height, depending on the Stokes number, St which can be defined near the midplane as

$$\text{St} = \frac{a \rho_m \pi}{\Sigma_g} \quad (2.5)$$

where ρ_m is the dust material density and under the assumption of Epstein regime and spherical particles (see Birnstiel et al. 2012). The dust-to-gas surface density ratio is 1/100 at all radii but varies along the altitude. The model does not include radial drift. The disk is composed of two separate dust populations, each with its own size, settling factor, and temperature structure.

2.2 Dust opacity

We adopt the standard size-averaged smoothed optical properties with the mixed mie coefficients used for the DSHARP project as described in Birnstiel et al. (2018). For each population, we use a size-averaged opacity derived from a dust grain size distribution following the MRN distribution with a power-law index $q = 3.5$. The small grain and large population have an upper grain radius of 1 μm and 1 mm, respectively. Both populations have a lower grain radius of 0.005 μm . The resulting dust absorption opacities, dust scattering and the g parameter of anisotropy are shown in Fig. 1. The disk thermal structure is computed using the Monte-Carlo radiative transfer code RADMC-3D and it is later post-processed using the gas-grain code NAUTILUS to obtain the evolution of the chemical abundances.

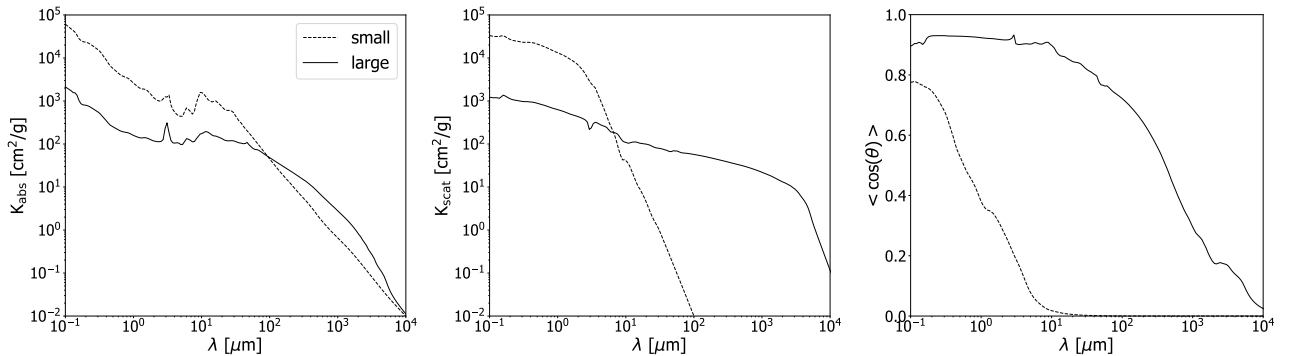


Fig. 1. Dust optical properties. **Left:** absorption coefficients. **Middle:** scattering coefficients. **Right:** Henyey-Greenstein g parameter of anisotropy ($g = \langle \cos(\theta) \rangle$).

3 Results

3.1 Thermal structure

Figure 2 shows the dust temperature radial profiles in the midplane. The small grains are warmer than the large grains of approximately 13 K at almost all radii, even in the midplane. Moreover, the small dust population temperature shows a surprising bump between ~ 30 au and ~ 80 au. Such temperature spread cannot exist in a model with a unique dust structure. This bump originates from the radiative interaction between the two populations: the scattered light from a grain species is absorbed by the other grain species. Note that the emission comes from the stellar light scattered from the upper layers.

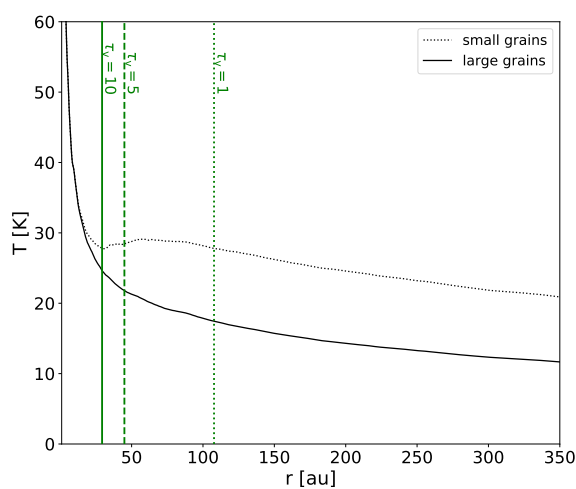


Fig. 2. Disk midplane radial profiles of dust temperatures. The black curves are the temperature profiles of the small grains (dotted line) and the large grains (solid line). The solid red curve is the temperature profile of a model with a single grain population. The vertical green solid, dashed, and dotted lines represent the radial distances from which the vertical optical depth (at $1 \mu\text{m}$) becomes smaller than 10, 5, and 1, respectively.

3.2 CO snowline

Figure 3 shows the CO ice adsorbed into each population separately. We see that the CO snowline for the small grains is located further away (~ 250 au) from the star because the grains are warmer than the large grains, whereas the snowline for the large grains is much closer (~ 25 au) because their surface is globally colder. Inside ~ 250 au, CO ice on the small grains is virtually non-existent because the temperature is above the freeze-out threshold for this population. There is thus a snowline segregation due to the presence of two temperature profiles. This, in principle, should affect the global chemical distribution in the disk. In particular, since the dynamical behaviour of the grains is also size-dependent, this could act as a segregated chemical delivery towards planetary embryos in more evolved disks.

4 Conclusions

We tested the impact of size-dependent vertical settling, dust densities, and dust opacities on the resulting dust temperatures and CO distribution in a protoplanetary disk model. We find that using different optical properties generates a systematic dust temperature spread, where the smaller grains are always warmer than the larger grains, in regions where the dust can be thermally decoupled. Most interestingly, the temperature of micron-sized grains can show a radial bump due to scattered stellarlight coming from the upper layers of the disk. The different temperatures affect the CO distribution in the disk because the CO condensation/evaporation balance is different from a grain species to another. The CO snowline is split since the temperature spread creates multiple condensation fronts. This effect does not require any radial drift process nor additional UV

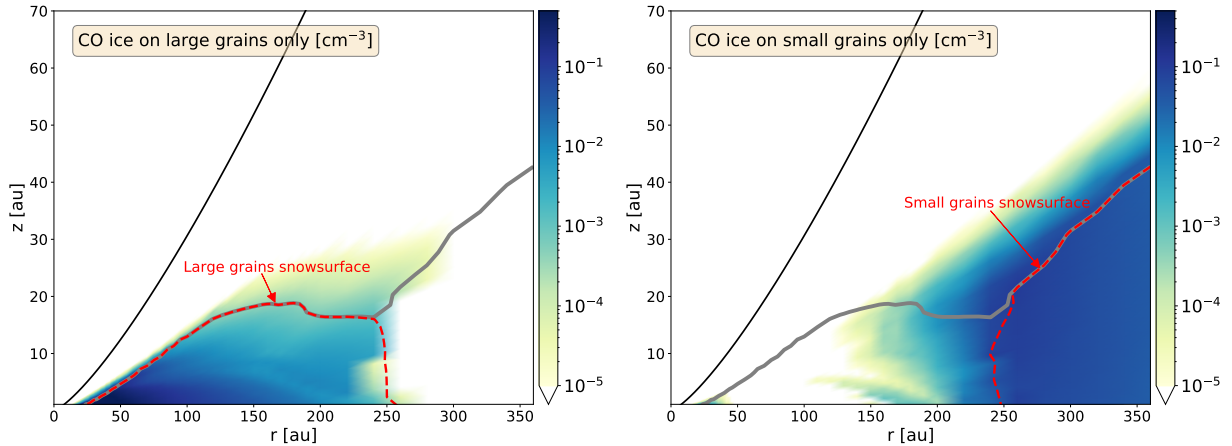


Fig. 3. 2-D maps of CO ice number density [cm^{-3}]. The solid grey line corresponds to the total CO snowline. The dashed red lines correspond to the snowline of each population independently. The black line is the maximum scale height below which chemistry is computed. **Left:** CO ice adsorbed onto the small dust population only. **Right:** CO ice adsorbed onto the large dust population only.

irradiation due to a change of dust-to-gas mass ratio, although radial drift should also reshape the CO snowline similarly. This result also shows that a size-dependent temperature has implication for chemical evolution during planet formation. Indeed, the formation pathway to more complex molecules via CO ice surface reactions is size-segregated. The small grains have virtually no CO ice on their surface inside the large grain snowline, and vice-versa, so that the formation of complex molecules via surface processes only occurs on the larger grains in the inner region of the disk, where planet formation is expected to take place. Later on, drifting pebbles from the outer disk, after the small grains have grown, should bring a different chemistry to the inner disk. Overall, this work suggests that it is not possible to create a 'fit-all' dust opacity model that can account for the dust temperature spread existing in a realistic size distribution.

S.G., J.K.J, and R.S acknowledge support from the Independent Research Fund Denmark (grant No. 0135-00123B). This work was supported by A. Dutrey and S. Guilloteau thank the French CNRS programs PNP, PNPS and PCMI. J. Kobus and S. Wolf acknowledge support from the DFG grant WO 857/19-1.

References

- Ballering, N. P., Cleaves, L. I., & Anderson, D. E. 2021, *ApJ*, 920, 115
 Birnstiel, T., Dullemond, C. P., Zhu, Z., et al. 2018, *ApJ*, 869, L45
 Birnstiel, T., Klahr, H., & Ercolano, B. 2012, *A&A*, 539, A148
 Dong, R., Zhu, Z., & Whitney, B. 2015, *ApJ*, 809, 93
 Du, F. & Bergin, E. A. 2014, *ApJ*, 792, 2
 Fromang, S. & Nelson, R. P. 2009, *A&A*, 496, 597
 Gavino, S., Dutrey, A., Wakelam, V., et al. 2021, *A&A*, 654, A65
 Gräfe, C., Wolf, S., Guilloteau, S., et al. 2013, *A&A*, 553, A69
 Harsono, D., Bjerkeli, P., van der Wiel, M. H. D., et al. 2018, *Nature Astronomy*, 2, 646
 Hersant, F., Wakelam, V., Dutrey, A., Guilloteau, S., & Herbst, E. 2009, *A&A*, 493, L49
 Ohashi, N., Tobin, J. J., Jørgensen, J. K., et al. 2023, *ApJ*, 951, 8
 Pérez, L. M., Chandler, C. J., Isella, A., et al. 2015, *ApJ*, 813, 41
 Testi, L., Birnstiel, T., Ricci, L., et al. 2014, in *Protostars and Planets VI*, ed. H. Beuther, R. S. Klessen, C. P. Dullemond, & T. Henning, 339–361
 Villenave, M., Ménard, F., Dent, W. R. F., et al. 2020, *A&A*, 642, A164
 Williams, J. P. & Best, W. M. J. 2014, *ApJ*, 788, 59
 Youdin, A. N. & Lithwick, Y. 2007, *Icarus*, 192, 588
 Zhang, K., Booth, A. S., Law, C. J., et al. 2021, *ApJS*, 257, 5